LABORATORY INVESTIGATION OF THE EFFECT OF VENUSIAN WEATHERING ON MINERAL SPECTRA. A. R. Santos[1], M. S. Gilmore[1], J. P. Greenwood[1], V. Tu[2] [1]Department of Earth and Environmental Sciences, Wesleyan University, Middletown, CT 06459 (asantos@wesleyan.edu), [2]Jacobs JETS, NASA Johnson Space Center, Houston, TX 77058.

Introduction: The recent selection of two missions to Venus has renewed the importance of determining weathering reactions between minerals and the Venusian atmosphere, and the spectral signatures of minerals before, during, and after these reactions. The rate at which weathering reactions progress also constrains how long unstable minerals will be present on the surface (e.g., [1]), and enables the use of mineralogy as a constraint on surface age (e.g., [2-3]). In order to gain an understanding of how mineral compositions and spectra change with weathering, we have begun conducting experiments in a 1 atm experimental setup at Wesleyan University. This setup exposes minerals to the temperature and most abundant gases of the Venus atmosphere (CO_2, SO_2, N_2). We conducted initial experiments using biotite, calcite, and montmorillonite in order to test our methodology with minerals that may be relevant to recording the history of water on Venus.

Methods: Experiments were conducted in Thermo Fisher Scientific Lindberg/Blue M Mini-Mite horizontal tube furnaces at Wesleyan University. Experiments used natural mineral chips and powders, and were conducted at 1 atmosphere and 460 °C under pre-mixed gases provided by AirGas (Table 1). The furnaces are set up in a flow through configuration so that solid samples are exposed to a fixed gas composition, and quartz glass process tubes were used in all experiments (1/4" diameter for experiment V4, ½" diameter for all others). These conditions were maintained for the durations listed in Table 1, at which point the furnace was turned off with gas flowing until the sample was cool enough to extract under N_2 and be placed in a desiccator for storage. Run products were carbon coated and examined using a Hitachi SU5000 Field Emission Gun Scanning Electron Microscope (SEM) equipped with an EDAX Octane Pro EDS detector located at Wesleyan University. Visible-Near Infrared Spectroscopy (VNIR) analysis was performed on powdered samples under a nitrogen atmosphere using an ASD Fieldspec Pro over the 350-2500 nm range. Powdered mineral samples were milled to a particle size of < 45 μm and were spiked with an internal standard (Al_2O_3, corundum) to obtain quantitative mineralogy. Samples were analyzed using a Panalytical X'Pert pro X-ray Diffractometer (XRD), with an X'Celerator high speed detector and Co Kα radiation, with data collected at a step size of 0.02˚/minute step counting rate from 2 to 80 degrees 2θ at 45 mA/40kV in the X-ray Diffraction Laboratory located at NASA Johnson Space Center. Materials Data Inc (MDI) software suite, Jade™ v9 was used for Rietveld refinement to determine phase abundances and mineral identification by comparing XRD patterns to International Center for Diffraction Data (ICDD) database patterns.

Table 1: Experimental matrix.

Experiment Name	Duration (Days)	Gas Composition (trace gas)	Minerals
V4	87	SO_2/N_2 (1.4%)	Montmorillonite, biotite
V5	19	SO_2/N_2 (1.4%)	Calcite
V6	19	$CO_2/SO_2/N_2$ (1.4% SO_2, 2.1% N_2)	Montmorillonite, biotite
V8	28	SO_2/N_2 (1.4%)	Biotite, calcite

Results: *Calcite*. In both experiments, calcite was exposed to the SO_2/N_2 gas mixture, and in both experimental run products, XRD analysis detected anhydrite, which is consistent with EDS measurements conducted in the SEM. The XRD analyses show greater amounts of anhydrite present after 28 days than 19, suggesting the calcite reaction progressed further given longer duration. Grain surface morphology as seen in the SEM also shows secondary mineral growth (Fig. 1). VNIR spectra show no change, as expected since anhydrite lacks spectral features in this wavelength range.

Montmorillonite. Montmorillonite was exposed to two different gas mixtures, the SO_2/N_2 mix and $CO_2/SO_2/N_2$ mix over different durations (87 and 19 days, respectively). VNIR analyses of both run products show a reduction in the 1441 and 1910 nm water features as well as a shift of the 1411 and 2011 nm features to shorter wavelengths that may indicate restructuring in the crystal lattice and the production of amorphous phases [4]. XRD results are consistent with this, showing a shift of the (001) peak from 15Å to 10Å in both run products. The amount of X-ray amorphous material in the montmorillonite run products was greater than that present in the unreacted clay, being the greatest in the 87 day V4 experiment. No other secondary phases were detected in the run products, however sulfur was present in EDS analyses of powder samples.

Biotite. Biotite was used in three experiments, one using $CO_2/SO_2/N_2$ gas (19 days), and two using SO_2/N_2 gas (28 and 87 days). In all three run products, XRD analysis detected phlogopite, suggesting the iron in biotite reacted with the gas, leaving behind an Mg-enriched mica. Amorphous material was also detected

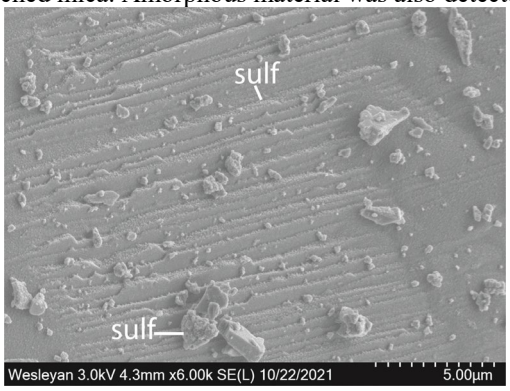

Figure 1: Secondary electron image of the surface calcite after a 19 day experiment under SO_2/N_2 gas. The entire mineral surface is covered in a secondary Ca-sulfate phase (sulf).

in the run product from the 87 day experiment only, suggesting that a secondary mineral of small grain size or poor crystallinity may have formed in the longer experimental duration. VNIR analyses show a reduction in the intensity of the 2333 nm (Fe^{2+} [5]) and 2397 nm (OH combination [6]) bands. Physical examination of the samples after experiment V6 indicate the presence of a magnetic phase, presumably magnetite. Despite this, examination under the SEM did not find significant Fe-oxides, but did find small Ca- and Na-sulfates forming from small particles on the surface of grains (Fig. 2). These elements are not major components of biotite, and likely either represent inclusions of another phase or impurities in the biotite chemistry.

Discussion: The observed reactions of minerals in these experiments largely followed predictions based on thermodynamic calculations and previous studies (e.g., [7]): Ca and Fe in minerals reacted with S and O gas species, and the clay mineral dehydrated. The two calcite experiments demonstrate the detection of reaction progress over time, as they used the same gas mix over different durations. This suggests our methods can be used to determine information about reaction rates.

The montmorillonite was largely effected by the temperature of the experiments, dehydrating as a result. This mineral also contains cations that tend to react with sulfur-bearing gases (e.g., Na, Ca), and the presence of sulfur in the montmorillonite run products suggests that these reactions may be happening, but discrete secondary mineral phases were not found.

The biotite experiments provide both an examination of experimental duration and effects of different gas mixtures. The amount of biotite remaining in the run product of the experiments using SO_2/N_2 gas decreases with time, suggesting more biotite has reacted. Interestingly, the amount of biotite remaining after only 19 days of exposure to the $CO_2/SO_2/N_2$ gas is less than that remaining after 28 days under SO_2/N_2 gas based on XRD analysis. This discrepancy may be indicating a difference in rate of reaction of biotite with different gas mixtures. Also interesting is the apparent sulfatization of Ca and Na in the biotite sample, elements that should be trace contaminants in biotite. The oxidation of Fe^{2+} in the biotite is in agreement with thermodynamic predictions from [8], and careful examination of future run products will determine what is happening to iron in this mineral.

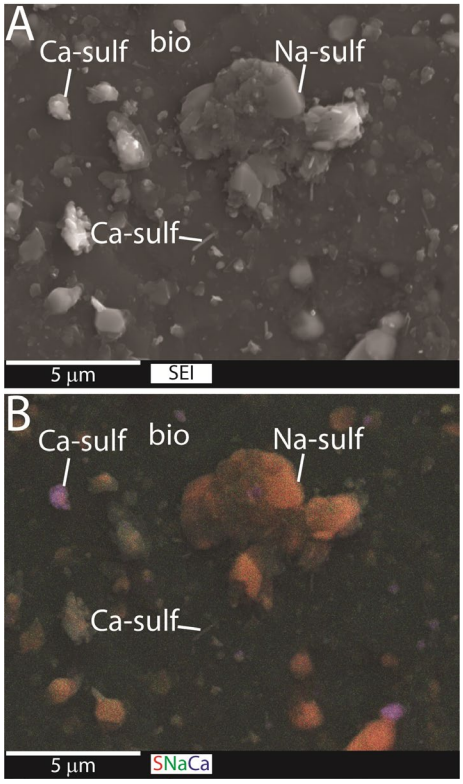

Figure 2: (A) Secondary electron image of the surface of biotite after 87 days under SO_2/N_2 gas. (B) An EDS element map showing distribution of S (red), Na (green), and Ca (blue) in the area shown in (A). Ca-sulf-calcium sulfate, bio-biotite, Na-sulf-sodium sulfate.

References: [1] Johnson N.M. and Fegley, B. (2000) *Icarus*, 146: 1, 301-306. [2] Smrekar S.E. et al. (2010) *Science*, 328: 5978, 605-608. [3] Filiberto J. et al. (2020) *Sci. Adv.*, 6: 1 eaax7445. [4] Che C. and Glotch T.D. (2012) *Icarus, 218*, 585-601. [5] Adams J.B. (1975) in *Infrared and Raman Spectroscopy of Lunar and Terrestrial Minerals* (C. Karr, Jr., ed), 91-116. [6] Bishop J.L. et al. (2008) *Clay Minerals, 43*, 35-54. [7] Zolotov M.Y. (2018) *RIMG 84*, 351-392. [8] Zolotov M.Y. et al. (1999) *Plan. & Space Sci, 47*, 1-2, 245-260.